Article ID: 1006-8775(2016) 02-0220-13

RELATIONSHIP BETWEEN THE VARIATION IN HORIZONTAL VORTICITY AND HEAVY RAIN DURING THE PROCESS OF MCC TURNING INTO BANDED MCSS

DING Zhi-ying (丁治英)[1], GAO Song (高 松)[1,2], CHANG Yue (常 越)[3]

(1. Key Laboratory of Meteorological Disaster, Ministry of Education / Joint International Research Laboratory of Climate and Environment Change / Collaborative Innovation Center on Forecast and Evaluation of Meteorological Disasters, Nanjing University of Information Science and Technology, Nanjing 210044 China;
2. Chongqing Institute of Meteorological Sciences, Chongqing 401147 China;
3. Guangzhou Meteorological Bureau, Guangzhou 510080 China)

Abstract: Using real-time data and the WRF mesoscale model, a heavy rain event in the process of Mesoscale Convective Complex (MCC) turning into banded Mesoscale Convective Systems (MCSs) during 18-19 June 2010 is simulated and analyzed in this paper. The results indicated that the formation and maintenance of a southwest vortex and shear line at 850 hPa was the mesoscale system that affected the production of this heavy rain. The low-vortex heavy rain mainly happened in the development stage of MCC, and the circular MCC turned into banded MCSs in the late stage with mainly shear line precipitation. In the vicinity of rainfall area, the intense horizontal vorticity due to the vertical shear of u and v caused the rotation, and in correspondence, the ascending branch of the vertical circulation triggered the formation of heavy rain. The different distributions of u and v in the vertical direction produced varying vertical circulations. The horizontal vorticity near the low-vortex and shear line had obvious differences which led to varying reasons for heavy rain formation. The low-vortex heavy rain was mainly caused by the vertical shear of v, and the shear line rainfall formed owing to the vertical shear of both u and v. In this process, the vertical shear of v constituted the EW-trending rain band along the shear line, and the latitudinal non-uniformity of the vertical shear in u caused the vertical motion, which was closely related to the generation and development of MCSs at the shear line and the formation of multiple rain clusters. There was also a similar difference in the positively-tilting term (conversion from horizontal vorticity to vertical positive vorticity) near the rainfall center between the low-vortex and the shear line. The conversion in the low vortex was mainly determined by $\partial v/\partial p<0$, while that of the shear line by $\partial u/\partial p<0$. The scale of the conversion from the horizontal vorticity to vertical vorticity was relatively small, and it was easily ignored in the averaged state. The twisting term was mainly conducive to the reinforcement of precipitation, whereas its contribution to the development of southwest vortex and shear line was relatively small.

Key words: heavy rain; Mesoscale Convective Systems (MCSs); numerical simulation; horizontal vorticity; twisting term

CLC number: P445 **Document code:** A

doi: 10.16555/j.1006-8775.2016.02.012

1 INTRODUCTION

Mesoscale Convective Systems (MCSs) are a type of strong convective system with intense convective precipitation that belong to the meso-β scale or meso-α scale. The Mesoscale Convective Complex (MCC) is the meso-α scale convective system with circular cluster structure which represents the extremity in the spectrum of MCSs. Domestic and international studies on the organized development process of MCSs have made many achievements (Meng et al.[1]; Cotton and Anthes[2]; Houze et al.[3]; Zhang and Fritsch[4]). As we all know, the formation of heavy rain, especially extremely heavy rain, requires relatively strong dynamic lifting conditions in addition to ample water vapor, and vorticity is a physical quantity that measures this dynamic condition. The vertical wind shear is accompanied by the accumulation and release of unstable energy that can generate horizontal vorticity, causing vortex motion in the flow fields around the horizontal axis. Based on the numerical model, Davies-Jones[5] noted that the rotation of horizontal airflow was related to the formation of updraft and downdraft during the motion of a thun der storm.

Received 2014-12-20; **Revised** 2016-01-24; **Accepted** 2016-04-15

Foundation item: National Program on Basic Research Project (973 Program) (2009CB421503, 2013CB430103); National Natural Science Foundation of China (40975037); Construction of Advantageous Disciplines for Higher Education in Jiangsu Province; Priority Academic Program Development of Jiangsu Higher Education Institutions (PAPD)

Biography: GAO Song, Engineer, primarily undertaking research on mesoscale meteorology and numerical simulation.

Corresponding author: DING Zhi-ying, e-mail: dingzhiying@nuist.edu.cn

Houze and Hobbs[6] found that such storms form a vortex tube around the horizontal axis due to the presence of vertical shear in the horizontal wind field, demonstrating that the horizontal vortex tube gradually turns into the vertical vortex tube due to the lifting of the updraft. This lifting implies the conversion from horizontal vorticity to vertical vorticity. As have been indicated in Chao and Chen[7], Moncrieff[8], Yan and Xue[9], Yu et al.[10], and Gao et al.[11], there is often dynamic instability in the vertical shear of a strong wind field that plays an important role in the organized development of MCSs to form large-scale heavy rain weather consequently. Studies of the Q vector and helicity have found that the horizontal vorticity can indirectly reflect the distribution of the vertical motion and the intensity of inflow in a thunderstorm. Therefore, it is important to analyze the role of horizontal vorticity in the formation and propagation of MCSs and the resulting vertical circulation and conversion to vertical vorticity. Many domestic and international research of horizontal vorticity focused on the intense convective system (such as squall lines and tornadoes), while studies on heavy rain processes were relatively few. The summer southwest monsoon in China easily forms a low-level jet stream and a rain band is to its north. There is often an accompanying upper-level jet stream to the north of the rain band. The vertical shear of these two directional winds produces the strong horizontal vorticity whose magnitude can be up to 10^{-3} s^{-1} near the jet. The main issues dealt with in this paper are how this strong horizontal vorticity affected the vertical circulation near the jet, the role of horizontal vorticity in the formation and reinforcement of heavy rain, and the relationship between the development of vertical vorticity and horizontal vorticity.

2 SYNOPTIC PROCESS CONTEXT

2.1 *Rainfall processes*

In June of 2010, there was a persistent heavy rainfall process in southern China, and Sichuan, Hunan, Jiangxi, and Fujian suffered severe floods. In particular, on June 18-20, due to the impact of a high-level trough and the eastward motion of a southwest vortex, there was large-to-heavy rainfall to the south of the Yangtze River and from west to east in southern China. The center of the heavy rain concentrated in the area from the mid-north of Jiangxi to the north of Fujian, where the rainfall was above 250-400 mm (Kong[12]). The heavy rain was caused by the activity of MCSs. From 0800 to 2000 June 19 (Beijing time), the heavy rain happened in Hunan, Jiangxi, and Fujian, and there was extremely heavy rainfall at some stations in Jiangxi and Fujian. During the process, the structure of the convective system was accompanied by the conversion from circular MCC to banded MCSs.

Therefore, we mainly analyze the rainfall process on June 18-19 in 2010 and simulate this process with numerical model. Based on the simulation results, we will focus the analysis on the horizontal vorticity during the conversion from MCC to banded MCSs and the impact of conversion from horizontal vorticity to vertical vorticity on the heavy rain to deepen our understanding of the mechanism of production of heavy rainfall in southern China.

2.2 *Circulation background and mesoscale systems*

According to the average large-scale circulation pattern at 500 hPa from 1200 UTC June 18 to 1200 UTC June 19 (Fig.1), there were a trough and a ridge at the mid-high latitude. The broad ridge area was located in the east of the Ural Mountains, and the trough area was located to the east of Lake Baikal. Near Liaodong Peninsula, there was a closed low-pressure center whose magnitude was up to 572 dagpm, and it exhibited a situation of high pressure in the west and low pressure in the east. There was a cold polar vortex near 70°N to the northeast of Lake Baikal. Inside the cold vortex, a steady southward stream of cold air gradually moved to the area south of Yangtze River and South China through the rear part of the northeast cold vortex. There was considerable short-wave trough activity on the straight band of westerly winds in the area to the mid-low latitude, which was conducive to guiding the eastward motion of the southwest vortex. The subtropical high was distributed in flat bands that shifted westward and became stronger, and the ridgeline was roughly located at 20°N. This arrangement caused the intersection of the warm air brought from the subtropical high with the cold air from the high-level trough, which was beneficial for the generation of severe precipitation.

Based on the analysis of the Temperature of Black Body (TBB) data, the convective cloud clusters in central-northern Sichuan started to merge from 0900 to 1200 UTC June 18 (Fig.2a). At 200 hPa, a divergence zone with a magnitude greater than 4×10^{-5} s^{-1} began to appear to the right side of the entrance of the upper-level jet stream (not shown), which corresponded to the initial stage of MCC cluster generation, and then the rainfall began. Meanwhile, there was a consistent incorporation of mesoscale convective cloud clusters in Sichuan Basin, and at 1800 UTC on June 18 (Fig.2b), the cloud clusters were located in the divergence area to the northeast of the South Asia high. From 2000 to 2300 UTC June 18 (Fig.2c), the intensity of merged cloud clusters increased to its strongest level, and the MCC entered the mature stage. The minimum value of TBB at the center was below −92℃, and the eccentricity was close to 1, which satisfied the definition of Maddox[13] for MCC. At 0000 UTC on June 19, the MCC was at its peak stage. The maximum divergence at the center was up to be 8.5×10^{-5} s^{-1} and was located directly behind the subtropical jet, which corresponded to a previous location with the development of MCC (not shown) and provided considerable upper-level divergence conditions for the rainfall to the south of jet. Next, the circular MCC gradually stretched eastward to become an

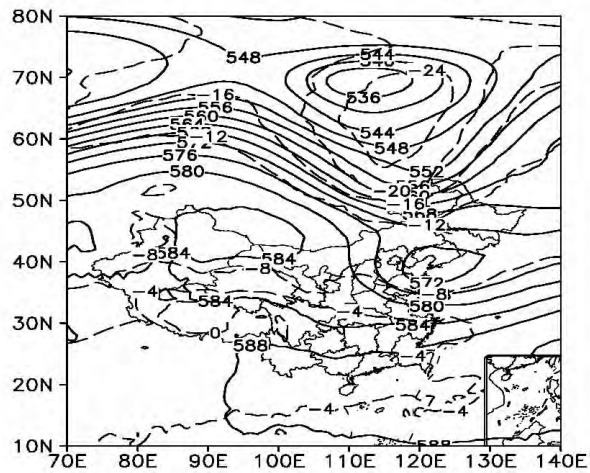

Figure 1. Average geopotential height field at 500 hPa between 1200 UTC June 18 and 1200 UTC June 19 (solid line; unit: dagpm) and temperature field (dashed line; unit:℃).

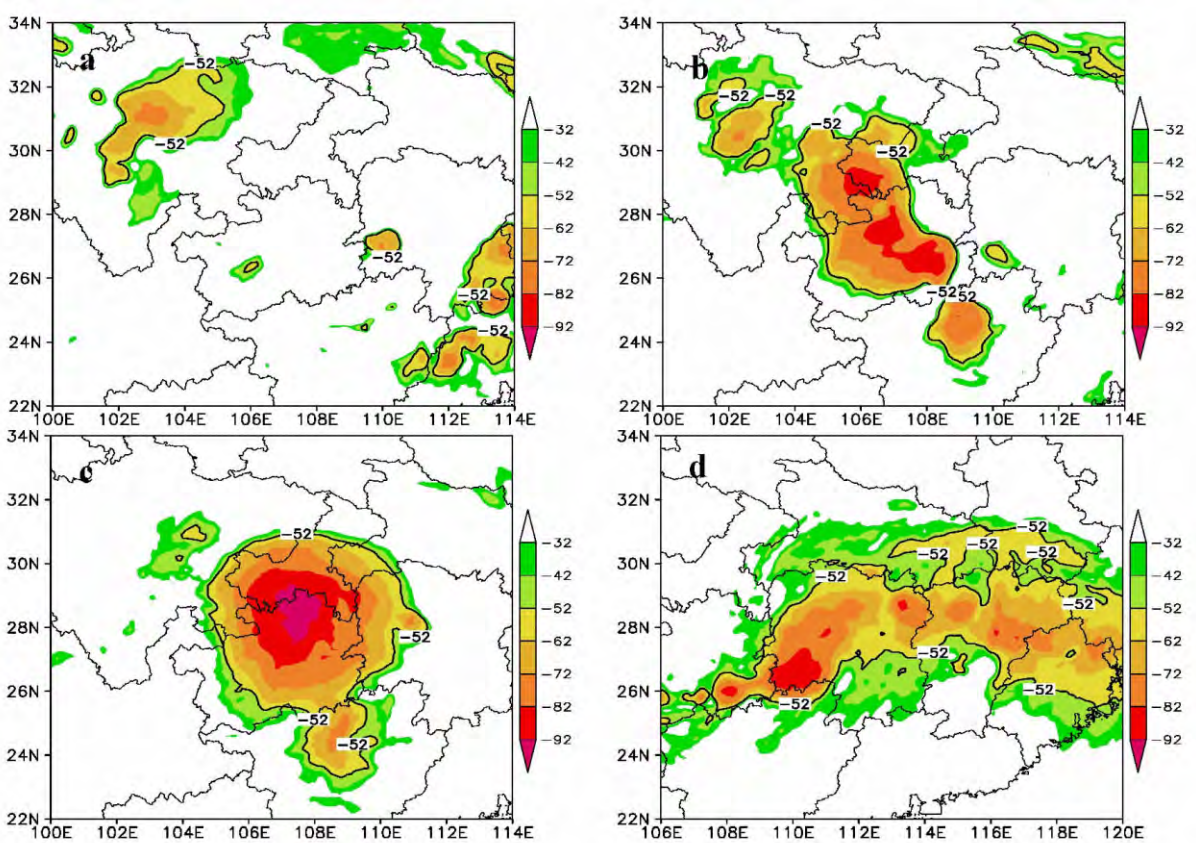

Figure 2. TBB distribution of FY-2E infrared cloud images (unit: ℃). (a) 1200 UTC on June 18; (b) 1800 UTC on June 18; (c) 2200 UTC on June 18; (d) 0900 UTC on June 19.

EW-stretching cloud band with multiple strong convective centers (Fig.2d). Correspondingly, the rain area and divergence area were both roughly distributed in bands from west to east with lots of strong rainfall clusters on the rain belt.

The analysis indicated that there was a close relationship between the formation of MCC and banded MCSs at the low level and the formation and eastward motion of the southwest vortex. It is known from the path of the southwest vortex that the center of the vortex was located in the west of Guizhou at 1200 UTC on June 18 (Fig.3a), and the low vortex then moved further northeastward along with the continuous development of MCC; at 0000 UTC on June 19, the southwest vortex was located in the north of Guizhou, and the shear line clearly extended eastward. The low-level jet stream be

came stronger, and multiple jet cores appeared. At this time, the entire South China was under the control of the low-level jet, and the northern cold air was strengthened. Simultaneously, there was a meso-β low vortex and a small meso-β high pressure near 117°E, 29.5°N, and 114°E, 31°N, respectively. Afterwards, along with the eastward motion of low vortex, the MCC elongated and evolved into banded MCSs, and the shear line rainfall reinforced (Fig.3b).

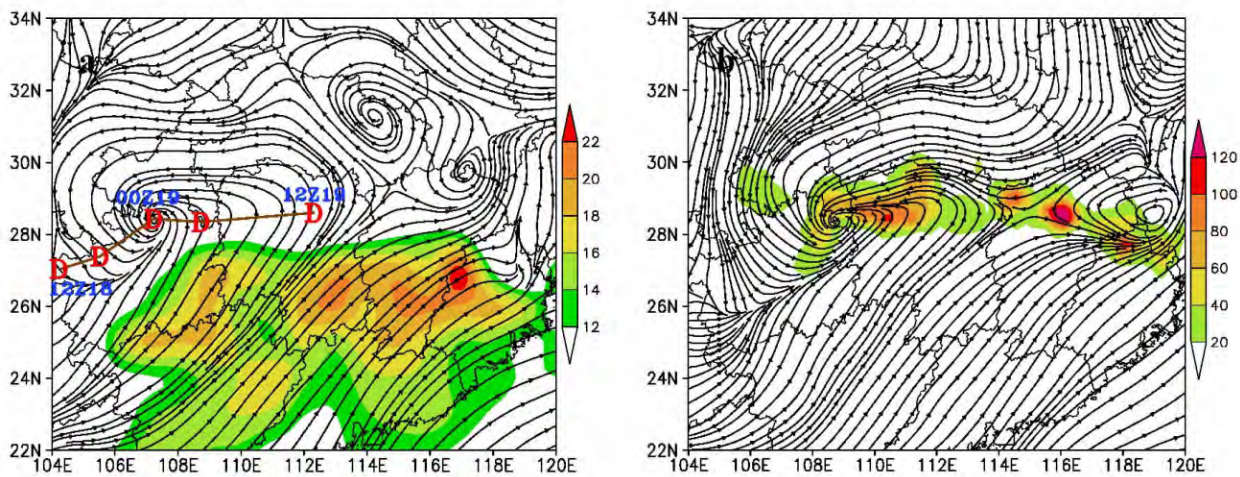

Figure 3. 850 hPa streamline field at 0000 UTC on June 19. (a) Shaded area for wind contours ≥12 m/s; eastward-moving path of the southwest vortex from 1200 UTC on June 18 to 1200 UTC on June 19 (solid line, where" D" is the location of the southwest vortex at 6 h intervals. (b) Streamline field at 0600 UTC on June 19 and the 6-h accumulated rainfall (shaded area; unit: mm).

3 DATA AND METHODS

In this paper, we used the non-hydrostatic mesoscale model (WRFV3.2.1) that was developed jointly by the U.S. National Center for Environmental Prediction (NCEP), U.S. National Center for Atmospheric Research (NCAR), and other U.S. research institutions for the numerical simulation of this event. The initial field and boundary conditions were provided by NCEP grid data with a resolution of 1°×1°. The physical schemes mainly included the following: the WSM6 microphysics scheme; the YSU boundary layer scheme; the Betts-Miller-Janjic cumulus parameterization scheme; the Noah land surface scheme; the RRTM long-wave radiation and Dudhia short-wave radiation schemes; and the GWDO parameterization scheme. The horizontal resolutions were 30 km and 10 km respectively. There were 28 layers in the vertical direction. The integration time of model was from 0000 UTC on June 18 to 1200 UTC on June 19. In this article, the hourly-output data at fine grids was used.

4 COMPARATIVE ANALYSIS OF THE SIMULATION AND THE OBSERVATION

The comparison between the 24-h simulated rainfall (Fig.4b) and the observation (Fig.4a) from 1200 UTC on June 18 and 1200 UTC on June 19 indicated that the position of simulated rain band was shifted southward by approximately 0.5 latitude degree compared with the observation. The distribution of the rain band corresponded to the real observation, and there were several centers of strong rainfall on the rain belt. In particular, the center of heavy rainfall at 117.8°E, 28°N was relatively close to that in the observation at 118°E, 27.8°N. The 24-h rainfall was greater than 200 mm, but the simulated position of two strong rainfall centers caused by a low vortex in the mid-north of Hunan was shifted southward by 1 latitudinal degree. The rainfall amount and range were both small. However, in general, the rainfall area, rainfall intensity, and trend of the rain bands in the simulation as well as the multiple rain clusters were all relatively consistent with the observation.

According to a comparative analysis of 850 hPa wind field at 0600 UTC on June 19 (Fig.5), the position of the southwest vortex was generally the same as the real observation. The excited meso-β low vortex was also reflected in the real field. The westerly and easterly shear line was near 29°N, which was consistent with the observation. The simulated low-level jet at 108°-112°E was weaker than in the observed conditions, which could be the reason that the rain band in this area shifted southward. The distribution of the jet, especially to the east of 113°E, was generally consistent with the observed conditions, and the rain bands were located between the easterly and westerly shear lines. In general, we simulated the generation and disappearance of rainfall areas and the rainfall strength, low vortex, and shear lines very well. The simulation of the systematic changes was also relatively accurate and could be used for further analysis.

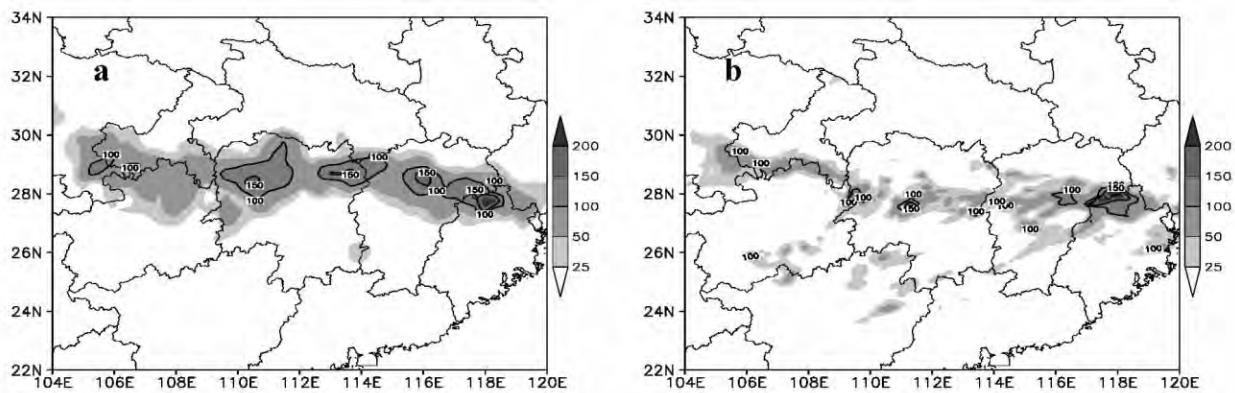

Figure 4. The rainfall amount (unit: mm) between 1200 UTC on June 18 and 1200 UTC on June 19. (a) observation; (b) simulation.

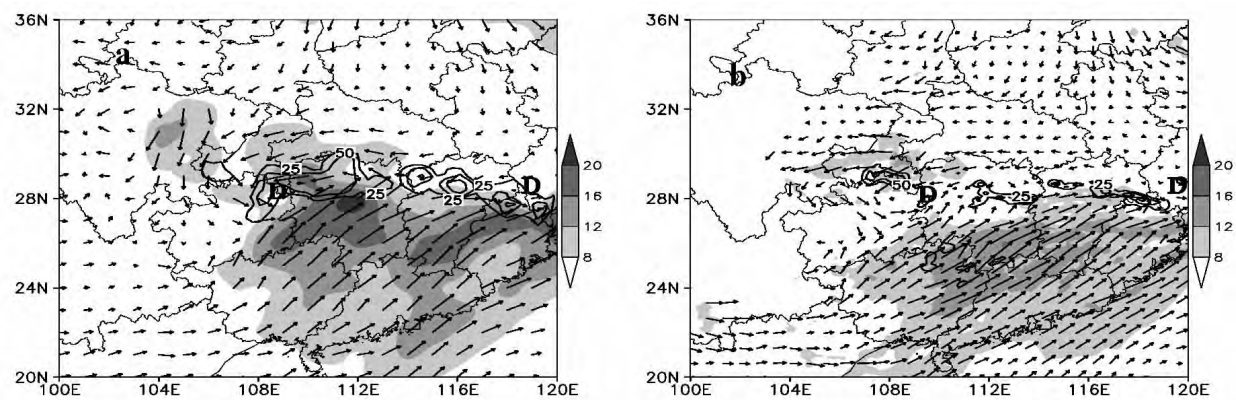

Figure 5. 850 hPa wind and low-level jet (shaded area; unit: m/s) at 0600 UTC on June 19: (a) observation; (b) simulation." D" is the location of the southwest vortex and meso-β low vortex; the contours are the 6-h accumulated rainfall for 0000-0600 UTC on June 19 (unit: mm).

5 RELATIONSHIP BETWEEN HORIZONTAL VORTICITY AND PRECIPITATION

Based on the definition of horizontal vorticity (Zhu et al.[14]), its component is

$$\zeta_x = \frac{\partial w}{\partial y} - \frac{\partial v}{\partial z}, \quad \zeta_y = \frac{\partial u}{\partial z} - \frac{\partial w}{\partial x}.$$

By analyzing the magnitude, its component of p coordinates can be written as

$$\zeta_x = \frac{\partial w}{\partial y} + \frac{pg}{R_d T}\frac{\partial v}{\partial p} \propto \frac{\partial v}{\partial p},$$

$$\zeta_y = -\frac{\partial w}{\partial x} - \frac{pg}{R_d T}\frac{\partial u}{\partial p} \propto -\frac{\partial u}{\partial p}.$$

where u, v, and w are the velocities in the x, y, and z directions, respectively, and ζ_x and ζ_y are the horizontal vorticities in the x and y directions, respectively.

During the development stage of MCC, at 2100 UTC on June 18 (Fig.6a), the rainfall near the southwest vortex corresponded considerably well with the area of the westward horizontal vorticity vectors. Correspondingly, as shown in Fig.6c, the area of low-vortex heavy rainfall corresponded to the center of negative ζ_x, and the minimum reached -14×10^{-3} s^{-1}. This matching indicated that the low-vortex heavy rainfall was mainly related to the vertical shear of v at that time. There was a southerly wind above 850 hPa and a northerly wind below (Fig.7c). After 0000 UTC on June 19, the banded MCSs developed and the southwest vortex weakened. The shear line extended eastward and there were multiple centers of strong precipitation, most of which located in the convergence zone of the horizontal vorticity vectors (figure omitted). At 0900 UTC on June 19 (Fig. 6b), the rainfall area exhibited a banded distribution, and the vorticity vector at the center of the strong rainfall generally pointed northwest (the distribution of ζy was clearly not uniform, which was related to the non-uniformity of the easterly and westerly perturbation in the vertical direction). To the south of the rain bands, there was mostly eastward horizontal vorticity vector, and the rainfall area to its north had a westward horizontal vorticity vector. In correspondence, the area of negative ζ_x in Fig.6d corresponded to the rainfall area, and to the south of rainfall area, there was mostly posi-

tive ζ_x. In the next section, we will focus the discussion on the dynamic process reflected by the horizontal vorticity vector and the reason for this type of relationship with rainfall.

According to the properties of horizontal vorticity such as the horizontal rotation caused by vertical vorticity, the presence of horizontal vorticity will inevitably cause rotation on the vertical cross section and thus cause the occurrence of vertical circulation. On the $y-p$ plane, the different variations in v with pressure cause variance in the circulation, and $\partial v/\partial p>0$ causes northern uplifting and southern downward sinking. For the same reason, on the $x-p$ plane, $-\partial u/\partial p>0$ can cause eastern downward sinking and western uplifting (because the x direction is affected by the basic jet, there is generally no latitudinal closed circulation), and vice versa. In the following, we denote the anti-clockwise circulation as positive circulation and the clockwise circulation as the anti-circulation (the same hereinafter). Therefore, the variation of v on the $y-p$ plane is the basis for the formation of longitudinal circulation or secondary circulation, or even circulation on smaller scales. The meeting of positive circulation and anti-circulation is conducive to rainfall formation in the common area of uplifting motion. This motion also explains why the rainfall was largest in the area with a positive ζ_x to the south of the shear line and a negative ζ_x to the north of it. In the $x-p$ plane, the updraft and downdraft caused by the non-uniform distribution of ζ_y are linked to the latitudinal formation of rain clusters. In the following, we will ana lyze the relationship between the horizontal vorticity and heavy rain during the low-vortex heavy rainfall stage and the shear line rainfall stage.

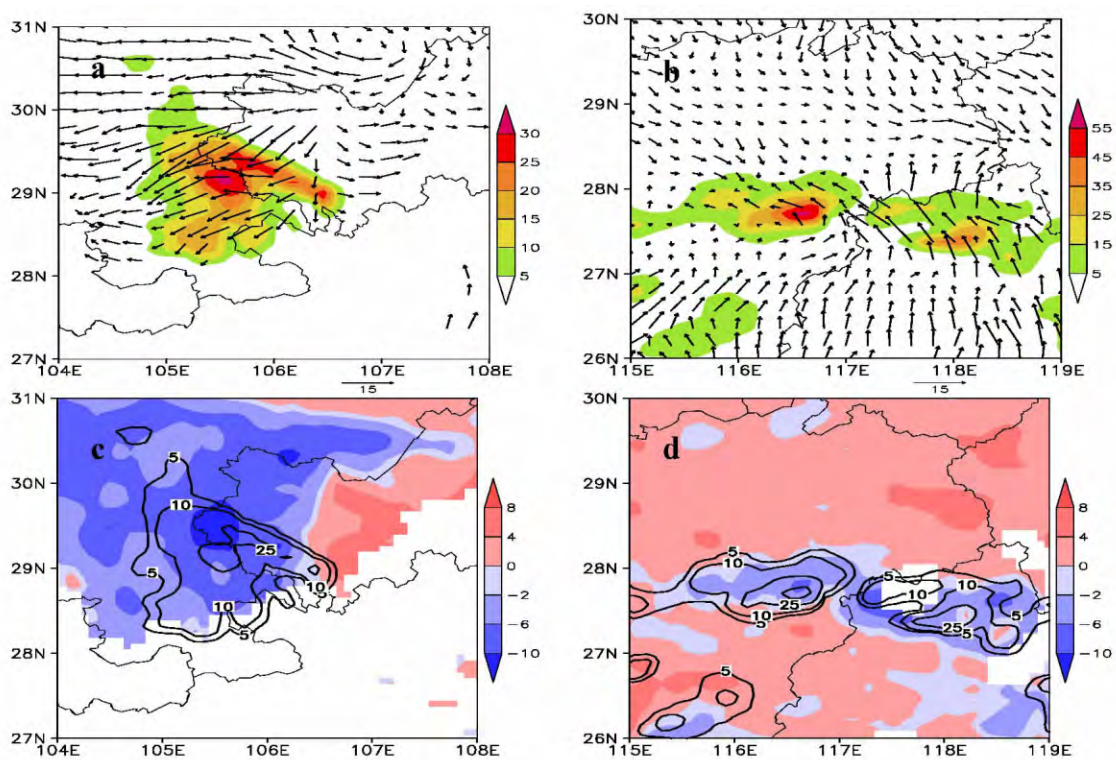

Figure 6. 850 hPa horizontal vorticity vector (vector, unit: 10^{-3} s^{-1}) and 1-h accumulated precipitation (shaded area; unit: mm) at (a) 2100 UTC on June 18 and (b) 0900 UTC on June 19. Distribution of 850 hPa ζ_x (shaded area; unit: 10^{-3} s^{-1}) and 1-h accumulated precipitation (solid line; unit: mm) at (c) 2100 UTC on June 18 and (d) 0900 UTC on June 19.

According to the analysis of the variation in the v component with pressures along the center of the low vortex (Fig.7a), at 1800 UTC on June 18, the region above the rainfall area was controlled by a northerly wind. There were two centers of northerly wind, and above them, there were another three centers of maximum southerly wind. The 600-350 hPa above the north of rainfall area near 31° N was the merged area of southerly and northerly winds, which formed a relatively strong north-south wind convergence. According to the analysis of the θe field, the southernmost of the front area reached 28° N. In Fig.7b, there are two clear anti-circulations at the two centers of the corresponding low-level north winds in Fig.7a that correspond to $\zeta_x<0$ and $\zeta_x>0$, and the upper level shows positive circulation. There was a northward tunnel between the upper-level positive circulation and the low-level anti-circulation, and the tunnel had a certain northward uplift. The uplifting area corresponded to the slope of the frontal area. Along the cross-section of the low-vorticity center at 2100 UTC on June 18 (Fig.7c), we found that the rainfall was considerably enhanced, and the centers of the

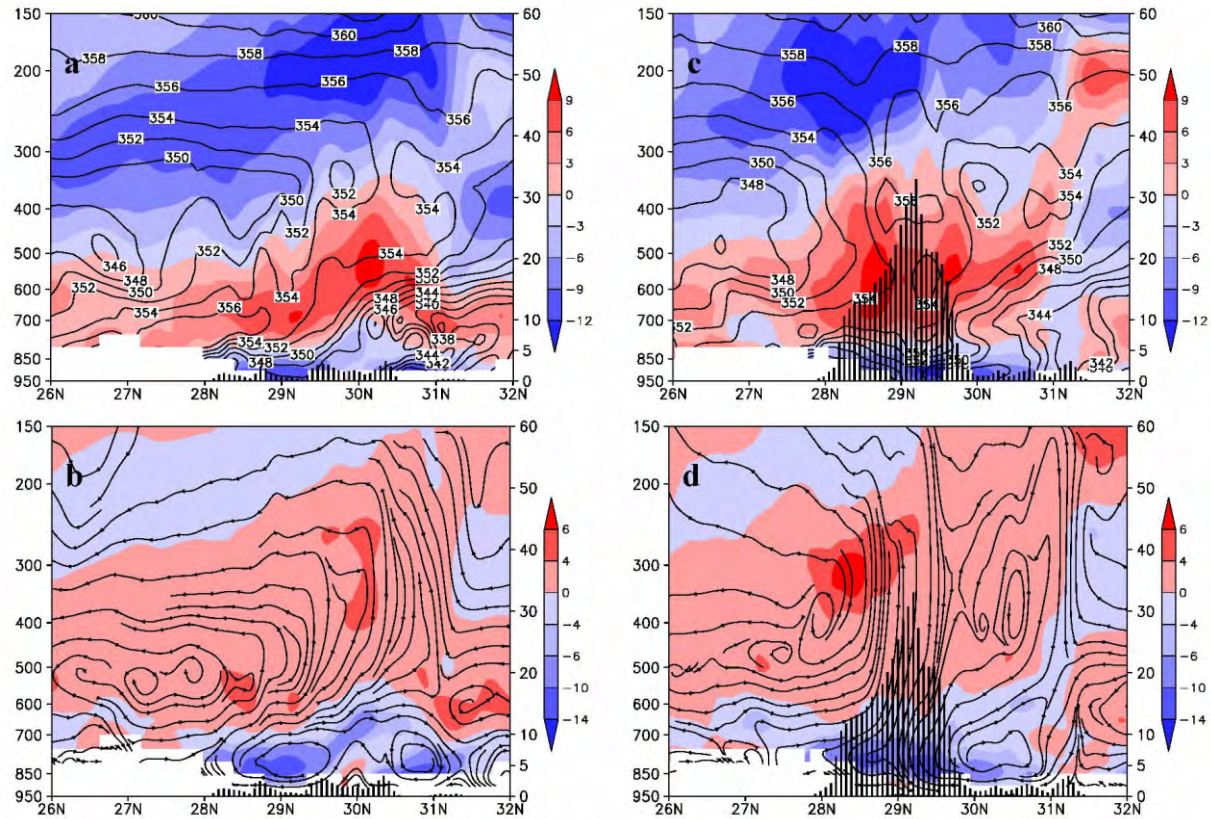

Figure 7. (a) Cross-section of the v component (shaded area; unit: m/s) and equivalent potential temperature (solid line; unit: K) along 105°E at 1800 UTC on June 18; (b) Cross-section of ζ_x (shaded area, unit: 10^{-3} s^{-1}, and the streamlines are the v–w circulation (w multiplied by 10) and the distribution of the 1-h accumulated rainfall (columns; unit: mm); (c) Cross-section of the v component along 105.5°E at 2100 UTC on June 18; (d) Cross-section of ζ_x, similar to panels a and b.

positive and negative v components above the rainfall area became larger, forming the center of the north wind with a speed >12 m/s at approximately 900 hPa; at the low level, the north wind moved southward to the south of 27°N. The area of the south wind at the middle level (600 hPa) was strengthened and uplifted to 50-100 hPa, and the center of the north wind at 200 hPa above 28.3°N was also enlarged. In Fig.7d, the center of the positive ζ_x greater than 6×10^{-3} s^{-1} formed at approximately 300 hPa above 28.3°N, and the horizontal vorticity became larger, forming a stronger vertical positive circulation. The north wind at the middle level north of the rainfall area was connected southward and down ward with the low-level north wind, causing the merging of the two centers of negative ζ_x at 1800 UTC on June 18, and the intensity was over -14×10^{-3} s^{-1}. It corresponded to the westward horizontal vorticity vector in Fig.6a, causing the strengthening of the low-level anti-circulation and forming the negative horizontal vorticity zone and the anti-circulation from the upper level to the low level to the right side of the heavy rainfall area to guide the southward motion of the cold air in the north. The tilted uplifting tunnel formed by the upper-level positive circulation and the low-level anti-circulation above the rainfall area constituted the rainfall-producing uplifting flow. At that time, the MCC became mature and was dominated by low-vortex heavy rain. The analysis showed that the anti-circulation caused by the vertical shear in the south and north winds on the side of the cold air and the positive circulation tunnel caused by warm air was the main reason for the low-vortex heavy rain. The low-level westward horizontal vorticity was linked to the activity of the cold air and frontal zone, and the strengthening process of ζ_x<0 indicated that the strengthening effect of the frontogenesis process on the formation of MCC and precipi tation.

After 0000 UTC on June 19, the shear line rainfall dominated to the east of 110°E, and the southernmost end of the front was generally maintained to the north of the rainfall area at approximately 28°N (Fig.8a). The 850-550 hPa was mainly controlled by a northerly wind, and the 550-200 hPa was controlled by a southerly wind. At the center of the southerly wind, $\partial v/\partial p$<0, and it was controlled by the area of negative ζ_x (frontal zone circulation) (Fig.8b). Therefore, there was a negative center at 850 hPa above the rainfall area, and the generated anti-circulation provided the uplifting airflow for the rain bands. This uplifting branch coincided with the uplifting branch of the positive circulation (circulation

formed by the southerly jet) generated by a positive ζ_x to the south of 28°N, which also proved that the coincidence of the ascending branch of the secondary circulation caused by the horizontal vorticity vector (westward to the north and eastward to the south of the rainfall area in Fig.6b) resulted in the enhancement of the rainfall. The variation in the circulation along the shear line was mostly similar. In Fig.8c, the shear line region was dominated by ascending motion, and the area of ascending motion was coordinated with a upper-level divergence area of the jet stream (not shown). The latitudinal distribution of the horizontal vorticity at approximately 200 hPa was not uniform, forming the latitudinal non-uniformity of the ascending and descending motions. Under 850 hPa, there was mainly $\zeta_y>0$, and above it there, were multiple centers, which also formed the latitudinal non-uniformity in ascending and descending motion. This indicated that the non-uniformity in the vertical shear of the easterly and westerly caused by the latitudinal upper-level and low-level jet streams was closely linked to the formation of multiple rain clusters.

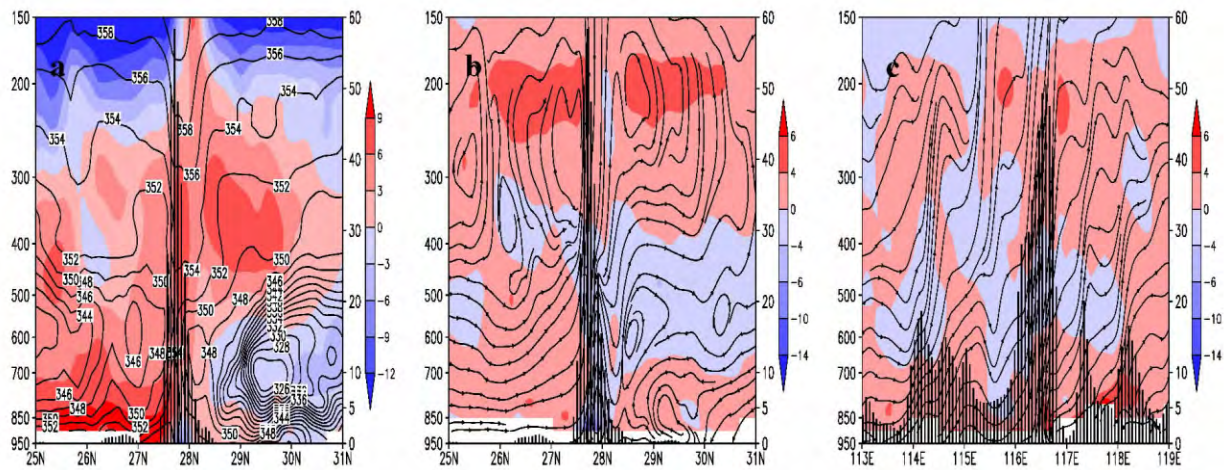

Figure 8. (a) Cross-section of the v component (shaded area; unit: m/s) and equivalent potential temperature (solid line; unit: K) along 116.6°E at 0900 UTC on June 19; (b) Cross-section of ζ_x (shaded area; unit: 10^{-3} s^{-1}, and the streamlines are the v–w circulation (w multiplied 10) and the distribution of the 1-h accumulated rainfall (columns; unit: mm); (c) Cross-section of ζ_y along 27.6°N (streamlines are the u–w circulation, and the description is the same as in panel b).

According to the analysis above, the vertical distri bution of the u and v fields is closely related to the horizontal vorticity and vertical circulation, and the horizon tal vorticity plays a critical role in the formation of the vertical circulation and heavy rainfall. The vertical circulation caused by the horizontal vorticity was also an important factor that triggered heavy rain. Meanwhile, the vertical circulation of the low vortex was considerably different from the circulation of the shear line. The mid-low level region with $\zeta_x<0$ was only accompanied by frontal area circulation, and the region with $\zeta_x>0$ was often accompanied by a low-level southerly jet. The $\zeta_y>0$ above the rainfall area was related to the non-uniform distribution of the vertical shear in the easterly and westerly caused by the latitudi nal upper-level and low-level jet streams. The MCC stage (low-vortex stage) was dominated by the influence of the frontal zone circulation, and the MCSs' stages (shear line stage) were controlled by the combined effects of the upper-level and low-level jet streams and the frontal zone circulation.

6 ANALYSIS OF THE VORTICITY BUDGET

Based on the analysis in the previous section, the horizontal vorticity had a significant impact on the circulation. However, what was the relationship between the horizontal vorticity and the vertical vorticity? How was horizontal vorticity converted to vertical vorticity in the area of heavy rain? Could horizontal vorticity affect the southwest vortex? Next, we will discuss these questions.

The vorticity budget is often used in the analytical study of cyclones and other systems (Liang and Li[15]; Zhang and Zhao[16]; Qiao et al.[17]), and the horizontal transportation of positive vorticity advection plays an indirect role in the development of surface cyclones. The total vortex source of the atmosphere is determined by the total contribution of four forcing terms. To analyze the relatively contribution of these four forcing terms to the vortex source, we calculated the distribution of the average vertical vorticity in the main rainfall area of the southwest vortex and the shear line and the budget of the 4 forcing terms in the vorticity equation.

The vorticity equation is as follows:

$$\frac{\partial \zeta}{\partial t} = M + N + P + R + S,$$

$$M = -[u\frac{\partial \zeta}{\partial x} + v(\beta + \frac{\partial \zeta}{\partial y})], \quad N = -\omega\frac{\partial \zeta}{\partial p},$$

$$P = -(\zeta + f)\nabla \cdot \vec{V}, \quad R = \frac{\partial \omega}{\partial y}\frac{\partial u}{\partial p} - \frac{\partial \omega}{\partial x}\frac{\partial v}{\partial p}$$

where M, N, P, and R are the horizontal advection term, vertical advection term, horizontal convergence and divergence term, and tilting term, respectively, and S is the friction term. Set W as the sum of the first four terms, and in the following discussion we neglect the impact of the friction term. Here, u and v are the latitudinal and longitudinal horizontal wind fields, ω is the vertical velocity, ζ is the vertical vorticity, f is the Coriolis parameter, and $\beta = \partial f / \partial y$.

At 1600 UTC on June 18, the southwest vortex had just formed during the development period of the banded mesoscale cloud clusters. At 1800 UTC on June 18, the MCC was at the developmental stage. From the distribution of the average vertical vorticity, it had a positive vorticity under 600 hPa, and the upper level had a negative vorticity (Fig.9a). In Fig.10a, under 600 hPa, P and N both contribute positively; between 750 and 500 hPa, the vorticity advection increased with height, which was conducive to the development of the low vortex, and there was a positive vorticity budget under the middle level. At 500-250 hPa, R and P contributed negatively, causing a negative vorticity budget; above 250 hPa, M contributed positively, and the negative vorticity budget turned into a positive vorticity budget, with the magnitude of M and W being essentially consistent. The tilting term in the figure was not a small term compared with the other terms during the development of the low vortex. Under 850 hPa, R converted to a positive vertical vorticity. Above it, there was mostly conversion to negative vertical vorticity, and the integration of the whole layer was negative.

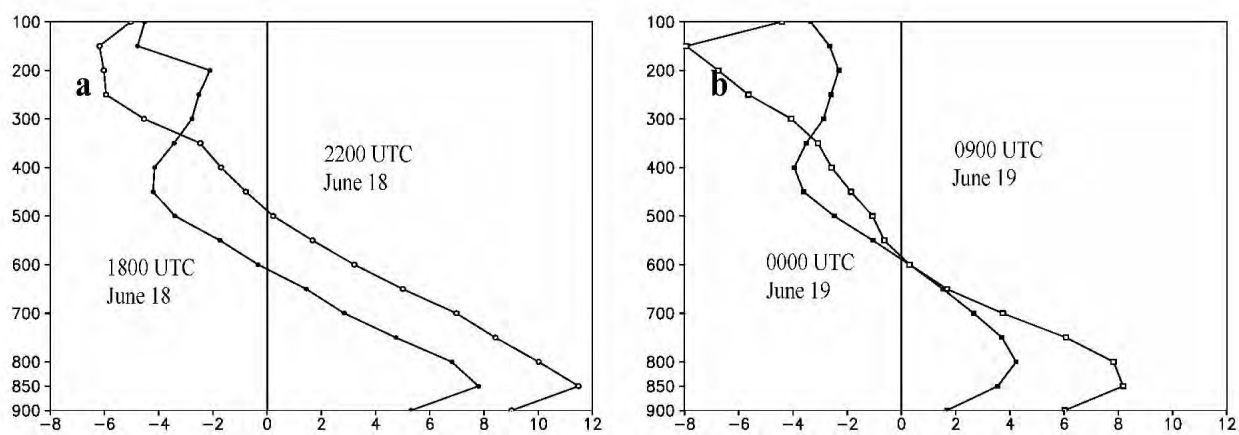

Figure 9. Distribution of regional average vertical vorticity at 1800 UTC (104°-106°E, 28°-30°N) and 2200 UTC on June 18 (105°-107°E, 28°-30°N) (a) and at 0000 UTC and 0900 UTC on June 19 (111°-119°E, 27°-28.5°N) (b) (unit: 10^{-5} s^{-1}).

At 2200 UTC on June 18, the MCC cloud clusters matured. Under 500 hPa, there was a deep distribution of positive vorticity that exceeded 10×10^{-5} s^{-1} at 850 hPa, and the negative vorticity at the upper level was strengthened (Fig.9a). The corresponding individual terms of the vorticity budget were strengthened during the developmental stage (Fig.10b). The range of 900-200 hPa had a deep positive vorticity budget. In particular, P and N had the largest contributions to the positive vorticity budget, and R had a relatively strong negative contribution to the vorticity budget. Especially at 600-300 hPa, N and the positive vorticity budget continued increasing, and the maximum vorticity budget reached 15×10^{-9} s^{-2}. Due to the vertical distribution of the vorticity advection that was negative below and positive above, according to the equation for vertical motion, the increase in the advection term for vorticity with height generated uplifting motion, which promoted the strengthening of the southwest vortex and strong development of the MCC, forming heavy rainfall.

After 0000 UTC on June 19, although the low vortex existed and there was rainfall nearby, the east was dominated by shear line rainfall. Therefore, we also analyzed the budgets of the individual terms in the vorticity equation near the shear line. 0000-0003 UTC on June 19 was the early stage of the shear line rainfall, and the vorticity variation in the whole layer was consistent with a low vortex, but the value was relatively small (Fig.9b). At this stage, the overall contribution of the vertical vorticity advection was relatively small. In general, the contribution of N and P to W was positive and the contribution of R and M was negative (Fig.10c). Later, the contribution of M increased. After 06 00UTC, the vorticity at the upper and low levels was stronger than during the early stages of shear line rainfall (Fig. 9b). At the stage with the strongest shear line rainfall (Fig.10d), the positive contribution of the N and P terms to W increased, and the tilting term R was mainly negative. There was a positive vorticity budget under 500 hPa. The M term increased from the low level to the middle level, while it decreased from the middle level to approximately 200 hPa. The negative vorticity budget at the upper level was mainly caused by R. This type of distribution promoted the development of a meso–β low vortex to the east of the low vortex and enhanced the shear line rainfall.

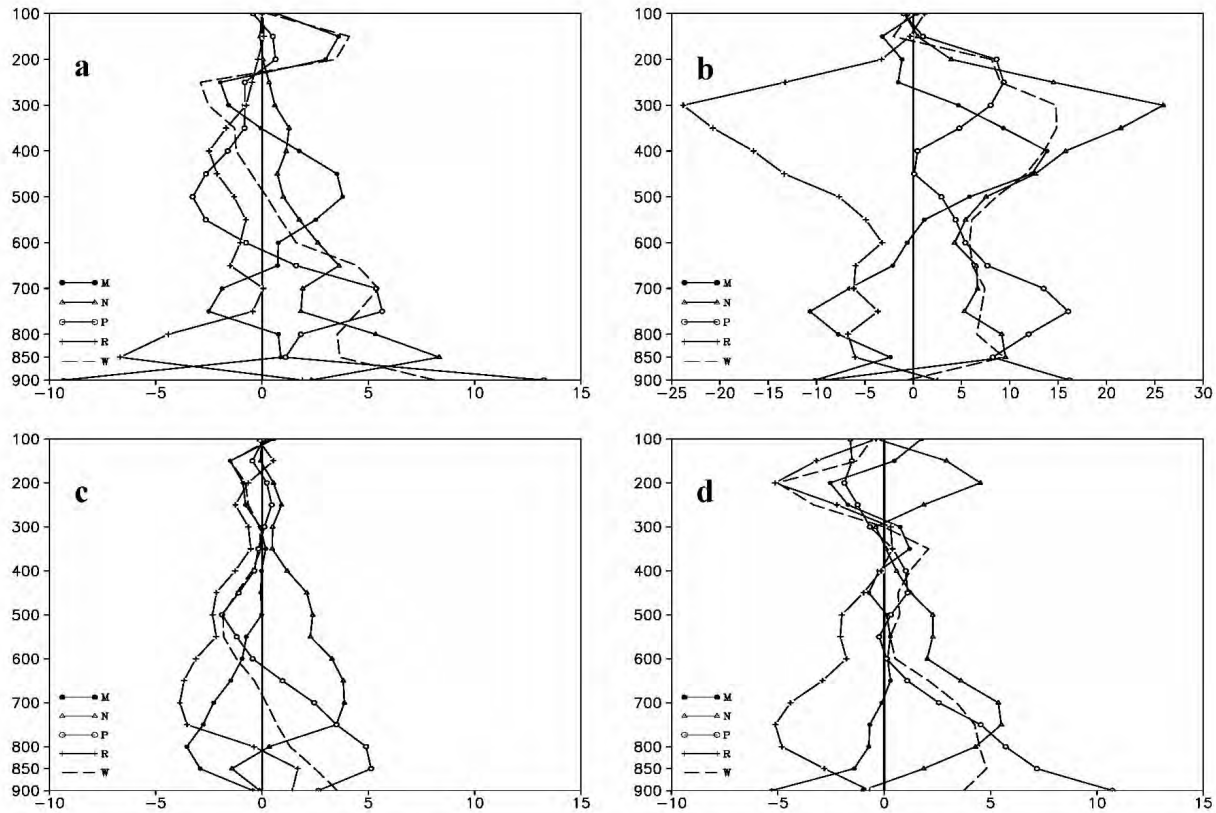

Figure 10. Vertical profile of the regional averages for the individual terms of the vorticity equation and the total vorticity budget (104°-106°E, 28°-30°N) at (a) 1800 UTC and (105°-107°E, 28°-30°N) at (b) 2200 UTC on June 18 and (111°-119°E, 27°-28.5°N) at (c) 0000 UTC and at (d) 0900 UTC on June 19 (unit: 10^{-9} s^{-2}).

According to the discussion above, the rotation of airflow in the vertical plane can cause a relatively strong horizontal vorticity. The contribution of horizontal vorticity to vertical vorticity should be relatively large, but why didn't the regional average demonstrate its role? As shown in Figs.11a and 11b, there was considerable conversion from horizontal vorticity and vertical vorticity in the low vortex and shear line rainfall areas at 850 hPa. However, the ranges of the positive and negative values were very small, and they were also similar to other figures, which indicated that the perturbation scale of this term was relatively small. This small scale could be the main reason that the contribution of the overall average to vorticity was relatively small. Because the vorticity vector is three-dimensional, the horizontal vorticity vector and vertical vorticity vector can be combined to better reflect the conversion from hori zontal vorticity to vertical vorticity. As shown in Fig. 11c, near 105.7°E with low-vortex heavy rain, there was a region of positive tilting term from the lower level to the middle level. The horizontal vorticity was converted to vertical vorticity due to the uplift of the vertical velocity. The mid-high level was mostly of negative vertical vorticity, and the tilting term was negative. In Fig. 11d, there was a region of positive tilting term at the lower level near 28°N vertical to the shear line, and the horizontal vorticity was converted to vertical vorticity. The middle region was mostly of negative vertical vorticity, and the vertical vorticity in the region of positive tilting term at 400-150 hPa was positive. We can see the conversion from horizontal vorticity to vertical posi tive vorticity. Apparently, the conversion near the low vortex occurred at the mid-low level, and the conversion near the shear line mainly occurred at the low level.

In summary, on the cross-section along certain longitudes or latitudes, the contribution of the tilting term to the vertical vorticity was relatively large, but is it possible that there is no universal significance due to the relatively small value? To answer this question, we analyzed individual terms (26 points for each) in the vorticity equation at the center of large tilting terms at 850 hPa at the low-vortex heavy rainfall stage (1200 UTC on June 18 to 0000 UTC on June 19) and the shear line rainfall stage (after 0000 UTC on June 19) (due to the presence of the low-level jet stream, the vertical shear was relatively large and thus it was reasonable to select the 850 hPa isobaric surface as the area of interest). The selection of these points was similar to the corresponding center of rainfall in Fig.11 (a and b), and we were mainly interested in studying the relative con tributions of the individual terms near the rainfall center. In Table 1, these points are superimposed. The table indicates that the largest term is the vorticity tilting term

rather than the vorticity advection term, followed by the convergence-divergence term and the vertical transportation term, and the smallest is the vertical vorticity advection term. Let $R_1=\frac{\partial\omega}{\partial y}\frac{\partial u}{\partial p}$ and $R_2=-\frac{\partial\omega}{\partial x}\frac{\partial v}{\partial p}$. Further analysis indicates that the R_2 term is much larger than the R_1 term for low-vortex heavy rain, and the R term is mainly determined by R_2. According to the magnitude analysis, the variations in ω in the horizontal direction were much smaller than the vertical shear of the horizontal winds, and in the region of $R_2>0$, $\partial\omega/\partial x$ was mostly greater than 0. Therefore, the magnitude of the R_2 term was mainly determined by $\partial v/\partial p<0$. According to the analysis in the previous section, $\zeta_x \propto \partial v/\partial p$, and the horizontal vorticity pointed westward, which was consistent with that; as shown in Fig.6a, the low-vortex heavy rain was mostly located in the westward horizontal vorticity. For the shear line rainfall, the R_1 term was much larger than the R_2 term, and the R term was mainly determined by R_1. In the region of $R_1>0$, $\partial\omega/\partial y$ was mostly smaller than 0. Therefore, the magnitude of the R_1 term was mainly determined by $-\partial u/\partial p>0$, while $\zeta_y \propto -\partial u/\partial p$ and the horizontal vorticity pointed northward, which was conducive to the formation of rainfall clusters in the x direction. This was consistent with the shear line rainfall being mostly located in northwestward horizontal vorticity (see Fig.6b).

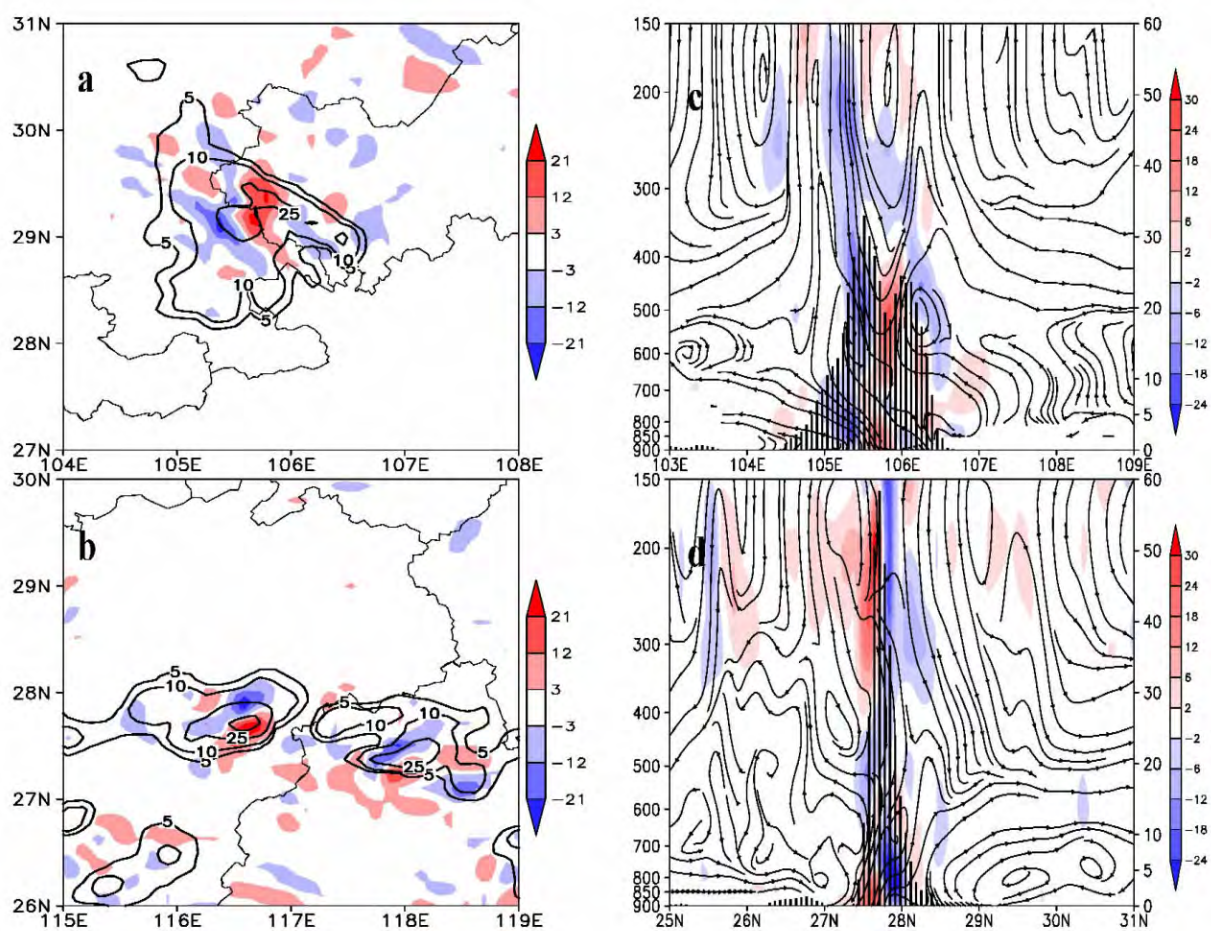

Figure 11. The tilting term (shaded area; unit: 10^{-8} s^{-2}) and the 1-h accumulated rainfall (contours, unit: mm) at 850 hPa at (a) 2100 UTC on June 18 and (b) 0900 UTC on June 19 and the cross-section of the R term (shaded area; unit: 10^{-8} s^{-2}) (c) along 29.2°N at 2100 UTC on June 18 and (d) along 116.6°E at 0900 UTC on June 19. The streamlines represent the vorticity vectors of $\zeta x-\zeta$, $\zeta y-\zeta$ (ζ multiplied 10) and the distribution of the 1-h accumulated rainfall (columnar area; unit: mm).

Table 1. The sum of the individual vorticity budgets at the center of the 26 largest values of the tilting term at the low vortex and shear line rainfall stages at 850 hPa (unit: 10^{-8} s^{-2}).

	Horizontal advection term (M)	Vertical transportation term (N)	Convergence-divergence term (P)	Tilting term (R_1)	Tilting term (R_2)	Tilting term (R)
Low vortex	-70.71	11.06	24.56	55.94	160.54	216.48
Shear line	-81.15	-59.33	126.35	277.19	84.39	361.58

Therefore, in the heavy rainfall area, the conversion of horizontal vorticity to vertical vorticity by the tilting term was crucial for the impact on heavy rain, which further indicated that the triggering effect of horizontal vorticity on heavy rain was not negligible. There was a considerable difference between the horizontal vorticity near the low vortex and the shear line. In the vorticity equation, if the scale of study is relatively small, then the regional average will ignore the factors with important influence on the precipitation.

7 CONCLUSIONS

This heavy rain event accompanied by MCC turning into banded MCSs was under the combined impacts of cold and warm air, the southwest vortex, and the upper-level and low-level jet streams. During the generation and development stage of MCC, the southwest vortex and heavy rain were generated. At the MCSs stage, the low vortex weakened, and the rainfall corresponded to the shear line. The maintenance of the low-level jet stream at 850 hPa and the coupling between the convergence zone to its left and the upper-level strong divergence field to its right, behind the upper-level jet at 200 hPa on the north side of the South Asia high, provided a good background for the generation of large-scale hor izontal vorticity.

The longitudinal and latitudinal horizontal vorticity generated by the vertical shear of the u and v wind fields is the main reason for the production of vertical circulation during the heavy rainfall process. During the development stage of MCC (the southwest vortex), the lower level was dominated by $\partial v/\partial p<0$, and the mid-high level was dominated by $\partial v/\partial p>0$. There was a north wind moving to the lower level to the north of the rainfall area that reinforced the frontal zone. During the MCSs stage (on the shear line), the south of the rainfall area was dominated by $\partial v/\partial p>0$, and the north of the rainfall (below 400 hPa) was dominated by $\partial v/\partial p<0$. The low level and upper level of the region near the rainfall area was the ascending area common to two circulations, which was conducive to the formation of rainfall, and $-\partial u/\partial p>0$ on the shear line was the main reason for the formation of the rain clusters. The generated ascending branch due to the rotation caused by the horizontal vorticity was also another important factor that triggered the heavy rain.

According to the regional average of the individual vorticities near the low vortex and the shear line, the increase in the advection term of the vertical vorticity with height was conducive to vortex development, and the tilting term was generally negative. The conversion from vertical vorticity to horizontal vorticity was not conducive to the development of the low vortex and the shear line. The positive tilting term near the center of the low-vortex and shear line rainfall (conversion from horizontal vorticity to positive vertical vorticity) was much larger than the other terms, and there was distinct deviation. The conversion of the low vortex was determined by $\partial v/\partial p<0$, and the conversion of the shear line was determined by $-\partial u/\partial p>0$. The non-uniformity of $-\partial u/\partial p>0$ distribution on the shear line was the main reason for the formation of the rain clusters. The low-vortex rainfall was mainly affected by the frontal circulation (produced by $\partial v/\partial p<0$), and the shear line rainfall was related to the non-uniformity of the vertical shear of the easterly and westerly caused by the upper-level and low-level jet streams. Therefore, the tilting term near the center of the low vortex, the shear line heavy rain that converted horizontal vorticity to vertical vorticity, and the circulation caused by the horizontal vorticity played a significant role in triggering the precipitation.

REFERENCES:

[1] MENG Wei-guang, ZHANG Yan-xia, DAI Guang-feng, et al. Analysis of formation and development process of a heavy rain mesoscale convective system in the coastal area of South China [J]. J Trop Meteorol, 2007, 23 (6): 521-530 (in Chinese).

[2] COTTON W R, ANTHES R A. Thunderstorm and Kinetic Mechanics [M]. Beijing: China Meteorological Press, 1993: 864-872 (in Chinese).

[3] HOUZE R A JR, RUTLEDGE S A, DIGGERSTAFF M I, et al. Interpretation of Doppler weather radar displays of mid-latitude mesoscale convective systems [J]. Bull Amer Meteorol Soc, 1989, 70 (6): 609-619.

[4] ZHANG D L, FRITSCH J M. Mathematical simulation of meso-β scale structure and evolution of 1977 Johnstown flood II: Inertially stable warm-core vortex and the mesoscale convective complex [J]. J Atmos Sci, 1987, 44 (18): 2 593-2 612.

[5] DAVIES-JONES R P. Tornado Dynamics. Thunderstorm: A Social and Technological Documentary [M]. KESSLER E (Ed), University of Oklahoma Press, 1980.

[6] HOUZE R A JR, HOBBS P V. Organization and structure of precipitating cloud systems [J]. Adv Geophy, 1982, 24: 225-316.

[7] CHAO Ji-ping, CHEN Li-shu. On the effects of the vertical wind shear on the development and the structure of convection [J]. Acta Meteorol Sinica, 1964, 34 (1): 94-102 (in Chinese).

[8] MONCRIEFF M W. Analytic representation of the large-scale organization of tropical convection [J]. J Atmos Sci, 2004, 21 (61): 1 521-1 538.

[9] YAN Jing-hua, XUE Ji-shan. Analysis of systematic structure of " 5.24" mesoscale heavy rain in South China with numerical simulation [J]. J Trop Meteorol, 2002, 18(4): 302-308 (in Chinese).

[10] YU Zhen-shou, GAO Shou-ting, REN Hong-xiang. A numerical study of the severe heavy rainfall associated with the typhoon" Haitang" [J]. Acta Meteorol Sinica, 2007, 65(6): 864-876 (in Chinese).

[11] GAO An-ning, LI Sheng-yan, CHEN Jian, et al. Feature analysis on extensive heavy rain process with weak environmental wind in western South China [J]. J Trop Meteorol, 2009, 25 (6): 9-17.

[12] KONG Qi. Analysis of the atmospheric circulation and weather on June 2010 [J]. Meteorol Mon, 2010, 36(9):

120-125 (in Chinese).
[13] MADDOX R A. Mesoscale convective complexes [J]. Bull Amer Meteorol Soc, 1980, 61 (11): 1 374-1 387.
[14] ZHU Qian-gen, LIN Jin-rui, SHOU Shao-wen, et al. Principle and methods of weather analysis [M]. Beijing: China Meteorological Press, 2007 (in Chinese).
[15] LIANG Bi-qi, LI Yong. The characteristics of the mesoscale environment and the cumulus feedback effects in a heavy rain [J]. J Trop Meteorol, 1991, 7 (1): 16-25 (in Chinese).
[16] ZHANG Feng, ZHAO Si-xiong. A dynamic study of low on Meiyu front producing heavy rainfall [J]. Clim Environ Res, 2003, 8(2): 143-156 (in Chinese).
[17] QIAO Feng-xue, ZHAO Si-xiong, SUN Jian-hua. Study of the vorticity and moisture budget of a northeast vortex producing heavy rain [J]. Clim Environ Res, 2007, 12(3): 397-412 (in Chinese).

Citation: DING Zhi-ying, GAO Song and CHANG Yue et al. Relationship between the variation in horizontal vorticity and heavy rain during the process of MCC turning into banded MCSs [J]. J Trop Meteorol, 2016, 22(2): 220-232.